Carbohydrate Polymers 134 (2015) 534–540

Contents lists available at ScienceDirect

Carbohydrate Polymers

journal homepage: www.elsevier.com/locate/carbpol

Isolation and characterization of cellulose nanocrystals from parenchyma and vascular bundle of oil palm trunk (*Elaeis guineensis*)

Junidah Lamaming[a], Rokiah Hashim[a,*], Cheu Peng Leh[a], Othman Sulaiman[a], Tomoko Sugimoto[b], Mohammed Nasir[a]

[a] *Division of Bioresource, Paper and Coatings Technology, School of Industrial Technology, Universiti Sains Malaysia, 11800 Minden, Penang, Malaysia*
[b] *Forestry and Forest Products Research Institute, 1 Matsunosato, Tsukuba 305-8687, Ibaraki, Japan*

ARTICLE INFO

Article history:
Received 8 June 2015
Received in revised form 23 July 2015
Accepted 7 August 2015
Available online 13 August 2015

Keywords:
Cellulose nanocrystals
Parenchyma
Vascular bundle
Morphological
Crystallinity
Thermal stability

ABSTRACT

In this study cellulose nanocrystals were isolated through acid hydrolysis process from parenchyma and vascular bundle of oil palm trunk (*Elaeis guineensis*). The morphological properties of obtained cellulose nanocrystals were studied by scanning electron microscopy (SEM) and transmission electron microscopy (TEM). The microscopy images showed smoother and cleaner surface of parenchyma cellulose nanocrystals when compared to vascular bundle cellulose nanocrystals. The TEM image shows a higher length and diameter for parenchyma cellulose nanocrystals compared to vascular bundle cellulose nanocrystals. The Fourier transform infrared (FTIR) spectra showed changes in functional groups after acid hydrolysis due to removal of lignin, hemicelluloses and other impurities in both type of cellulose nanocrystals. Crystallinity index of cellulose nanocrystals was observed higher for vascular bundle as compared to parenchyma. Thermogravimetric analysis (TGA) was performed to study the thermal stability of cellulose nanocrystals and it was observed higher for parenchyma cellulose nanocrystals compared to vascular bundle.

1. Introduction

As a valuable, sustainable and perennial cash crop, oil palm industry contributes a major role in Malaysia's economy. However, the oil palm trunks are considered useless and left behind to rot or burnt in the field. Although, a huge amount of oil palm trunk (OPT) is produced every year, it remains unused due to its own demerits such as low density, high hygroscopicity and lower dimensional stability. If, the OPT is processed well and modified intelligently, it can be a huge source of alternative wood for various non-structural materials in the packaging and furniture industries.

The trunks are composed of vascular bundle and parenchymatous tissue which act as transporting and food storage organs, respectively (Corley & Tinker, 2003). Fig. 1 illustrates a simple structure of oil palm trunk studied by Hashim et al. (2012). The outer part is mostly composed of vascular bundle, provides mechanical support and help in transporting water and nutrients (Corley & Tinker, 2003) whereas the central part is composed of 70% of parenchyma cortex tissue (Bakar et al., 2012). The density of vascular bundles increased from the lower to the top of the oil palm which decrease gradually toward the central zone (Lim & Khoo, 1986). These vascular bundles are slightly larger and widely spread as they are embedded in the thin-walled of parenchymatous ground tissues. The vascular bundles found toward core side are larger in size and widely scattered. The number of vascular bundles determines the density and mechanical properties of the oil palm trunk (Bakar et al., 2012; Darwis et al., 2013).

The vascular bundles are characterized as dense, fibrous and least hygroscopic whereas the parenchyma cells are soft, spongy, and highly hygroscopic in nature (Killmann & Lim, 1985; Abe et al., 2013). However, the vascular bundle is much less densely packed toward the central zone where more of the storage tissue is located. The vascular bundle is composed of fibers, xylem, vessels, protoxylem, sieve tubes, axial parenchyma, stegmata and companion cells (Lim & Fujii, 1997; Sulaiman et al., 2012; Abe et al., 2013). Abe et al. (2013) added that a living parenchyma cells store the food as carbohydrate, mostly in the form of sugars and starch. The ground parenchymatous tissue is consisting of thin-walled spherical parenchyma cells, which is highly dense and thick in the core region as compared to the outer region. Cell division and elongation in the parenchymatous ground tissues as well as vascular fiber lead to growing in diameter and length of oil palm trunk (Killmann & Lim, 1985; Sulaiman et al., 2012).

* Corresponding author. Tel.: +60 4 653 5217; fax: +60 4 6536375.
E-mail addresses: hrokiah@usm.my, hrokiah1@gmail.com (R. Hashim).

http://dx.doi.org/10.1016/j.carbpol.2015.08.017
0144-8617/

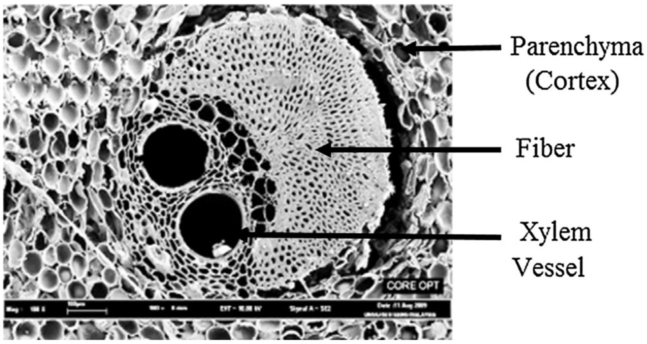

Fig. 1. Anatomical structure of oil palm trunk studied by Hashim et al. (2012).

The OPTs are rich in parenchyma cell which holds more moisture than vascular bundles. The parenchyma tissue provides hydroxyl groups that can help in retaining more water molecule by hydrogen bond formation. Furthermore, the trunk itself is composed of parenchyma and vascular bundle having extractives (19.05% and 15.33%), lignin (20.71% and 11.91%), and holocellulose content of 77.38% and 82.38% (Lamaming, Hashim, Leh, Sulaiman, & Sugimoto, 2015a), respectively. The high amount of parenchyma and vascular bundle in OPT can be exploited as a potential future source for cellulose nanocrystals production.

However, several research have been done dealing with the micro-structure of oil palm trunk and provide a useful knowledge to utilize it for various purposes (Mhd Ramle et al., 2012; Prawitwong et al., 2012; Abe et al., 2013) but isolation of cellulose nanocrystals from parenchyma and vascular bundle of oil palm trunks has not been reported yet. Although, a detailed study of anatomical features on oil palm trunk such as characterization of parenchyma and vascular bundle was carried out in our previous work (Lamaming et al., 2015a) but the cellulose nanocrystals were extracted from OPT without separating parenchyma and vascular bundle (Lamaming et al., 2015b). Therefore, in this study cellulose nanocrystals were extracted separately from parenchyma and vascular bundle of oil palm trunk and their characteristic properties were investigated. The result obtained from this research would be useful in near future for potential applications in specified field such as in medicals.

2. Materials

2.1. Samples preparation

The oil palm trunk, collected from Kuala Selangor was debarked, cut and chipped into smaller chips of size 4–5 cm before drying into the oven at 50 °C. The dried OPTs were pounded, and parenchyma and vascular bundle were segregated manually as can be visualized in Fig. 2. The segregated parenchyma and vascular bundle were grounded into powder form before de-waxing in ethanol: toluene (2:1, v/v) for 6 h. The fibers were filtered and dried at 50 °C and stored in sealed container.

2.2. Cellulose nanocrystals isolation

The method to prepare the cellulose nanocrystals was as described in our previous work (Lamaming et al., 2015b) following the procedure done by Fahma, Iwamoto, Hori, Iwata, and Takemura (2010). Briefly, the parenchyma and vascular bundle powder of oil palm trunk were bleached using sodium hypochlorite ($NaClO_2$) under acidic condition (acetic acid pH 4–5) at 70 °C for 3 h. The washed fibers were then soaked in 6% potassium hydroxide (KOH) for 24 h at 20 °C and rinsed with deionized water until the pH was neutral. The resulting cellulose was hydrolyzed with 210 ml of 64% sulfuric acid (H_2SO_4) at 45 °C for 1 h. After terminating the hydrolysis with the addition of 400 ml of cold water, the diluted suspension was centrifuged then dialyzed for a few days until reached constant pH.

2.3. Methods

2.3.1. Field emission scanning electron microscopy (FESEM)

The morphology of parenchyma and the vascular bundle was analyzed using FESEM micrographs with an LEO Supra 50 Vp FESEM with ultra-high resolution. The samples were coated with gold using Polaron SC 515 ± 20 nm sputter coater to avoid charging.

2.3.2. Transmission electron microscopy (TEM)

Samples for transmission electron microscopy were observed with a Philips CM12 electron microscope. Cellulose nanocrystals of parenchyma and vascular bundle in water suspension were sonicated for a few minutes before dropping and depositing the diluted suspension from each sample into the carbon-coated grid. The sample was stained and allowed to dry before viewed under the microscope. A total of 20 fibers of each sample were measured by their diameter and length.

2.3.3. Fourier transformed infrared (FTIR) spectroscopy

The FTIR spectra of parenchyma and vascular bundle cellulose nanocrystals were recorded using Thermo Scientific model Nicolet I S10 spectrometer. Dried powder of parenchyma and vascular bundle cellulose nanocrystals were pounded together with KBr and pressed into a pellet. The pellet was then viewed in the spectrometer in the range from 500 to 4000 cm^{-1}.

2.3.4. X-ray diffraction (XRD)

An X-ray generator with Cu$K\alpha$ radiation (λ = 1.5406 Å) generated at a voltage of 45 kV and current of 30 mA was used to characterize the crystalline structure of the nanocrystals isolated. All samples were scanned in 2θ ranges varying from 5 to 50°

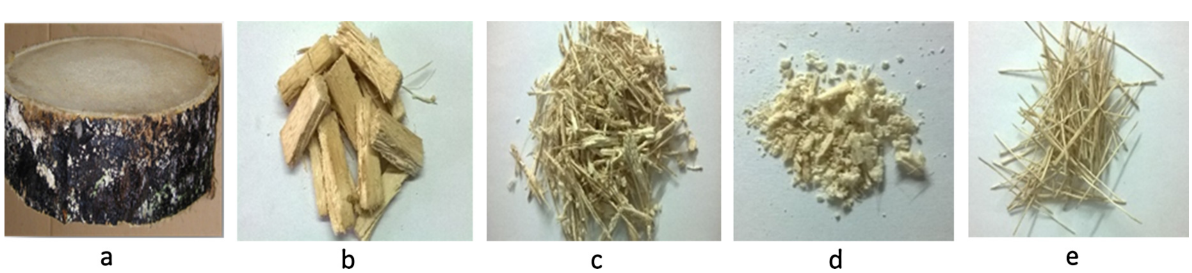

Fig. 2. (a) Oil palm trunk disc (b) chipped oil palm trunk (c) pounded oil palm trunk (d) parenchyma (e) vascular bundle.

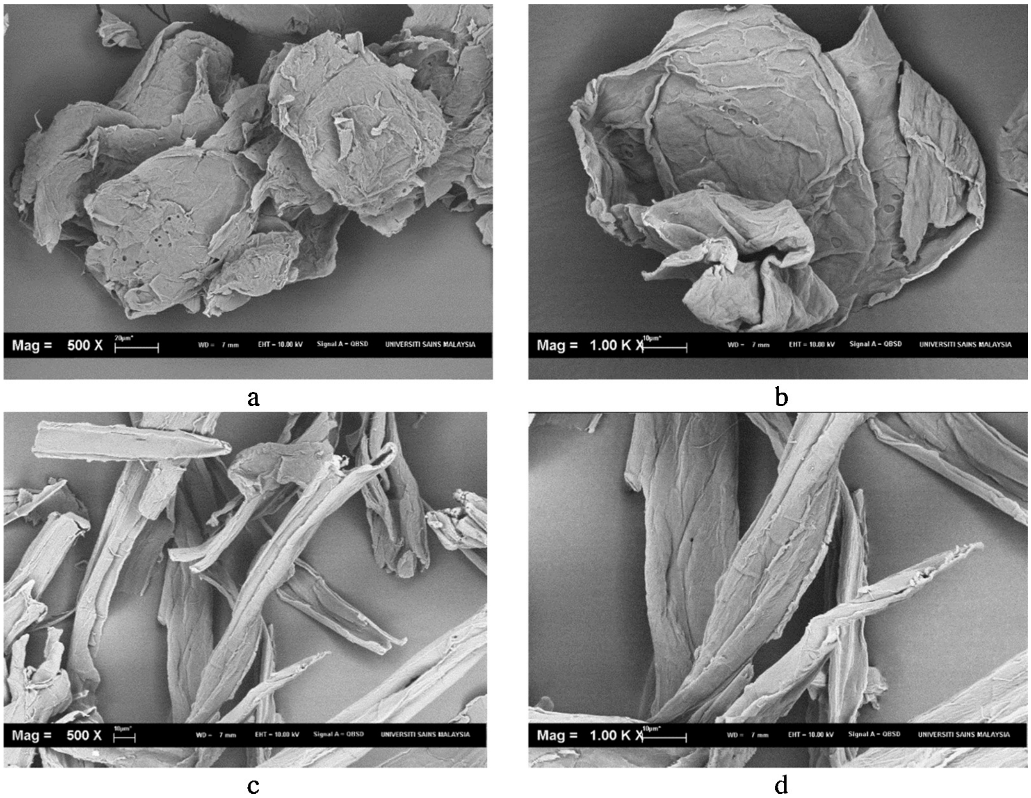

Fig. 3. SEM micrographs of oil palm trunk (a) parenchyma (×500), (b) parenchyma (×1.00 K) and (c) vascular bundle (×500), and (d) vascular bundle (×1.00 K) after chemo-mechanical treatment.

at 2°/min. The crystallinity index was calculated based on Segal, Creely, Martin, & Conrad (1959) the following equation:

$$C_{Ir}(\%) = \frac{(I_{002} - I_{am})}{I_{002}} \times 100 \quad (1)$$

where I_{002} is the peak intensity corresponding to crystalline ($2\theta = 18°$) and I_{am} is the peak intensity of the amorphous region ($2\theta = 22°$).

2.3.5. Thermogravimetric analysis (TGA)

Thermogravimetric measurements of cellulose nanocrystals from parenchyma and a vascular bundle of oil palm trunk were performed by using Perkin Elmer Pyris 1 thermogravimetric analyzer. Each sample was scans at 30 to 800 °C with a rate of 10 °C min^{-1} in a nitrogen atmosphere.

3. Result and discussion

3.1. Morphological studies

Fig. 3 displays the micrographs of parenchyma and vascular bundle after chemo-mechanical treatment. From Fig. 3c and d, it was observed that the fibers of the vascular bundle are thicker than parenchyma (Fig. 3a and b). According to Mauseth (1988) and Pruyn (2007), the parenchyma cells are very thin and considered as feeble cells when compared to the thick walls of fiber cells. The cell shape is formed probably due to the result of surface tension and/or pressure from surrounding cells. As the vascular bundle are found more in the outer zone of the trunks compared to the central zones, the fiber becomes shorter and having a smaller diameter and thicker cell walls. These thick wall vascular fibers in oil palm trunk contribute higher cellulose content which is directly proportional to the strength. The chemo-mechanical treatment removes the starch, lignin, hemicelluloses and other impurities from OPT fibers, thus the parenchyma cell, and vascular bundle looks smooth and clean.

Fig. 4 displays the TEM images of the cellulose nanocrystals of parenchyma and vascular bundle, segregated from oil palm trunk. From the figure, the individual fiber can be studied. Cellulose nanocrystals from parenchyma shows a higher length and diameter, 892.86 nm and 10.51 nm compared to cellulose nanocrystal from the vascular bundle that is 176.20 nm and 4.28 nm, respectively. This is probably due to the shortening of fibers during the grinding process that showed vascular bundle fibers are easily broken compared to parenchyma cells. The vascular bundle fiber is long while the parenchyma is in spherical shape. Therefore, when putting the vascular bundle and parenchyma in the grinder, the vascular fiber that is long is easily to break compared to the spherical shape of parenchyma.

3.2. Fourier transform infrared analysis

The FTIR identifies the functional groups that are present in the sample. As a lignocellulosic material, oil palm trunk parenchyma and vascular bundle composed mainly of hemicelluloses, lignin and celluloses. Therefore, alkanes, esters, aromatics, ketones and alcohols with the different oxygen-containing functional group are the main composition of these materials (Abraham et al., 2011). Fig. 5 displays the FTIR spectra of parenchyma and vascular bundle cellulose nanocrystals. The spectra of both the cellulose nanocrystals showed a similar peak and resembles with our previous work on cellulose nanocrystals obtained from oil palm trunk (Lamaming et al., 2015a,b). The peak at 3406 cm^{-1} and 3355 cm^{-1} in the parenchyma and vascular bundles, respectively, were attributed to the intensity OH groups, which is found higher for parenchyma. The high intensity of OH group in parenchyma makes it more hygroscopic as stated by Abe et al. (2013). The peak at 1641 cm^{-1} represents the OH bending of absorption of water. According to

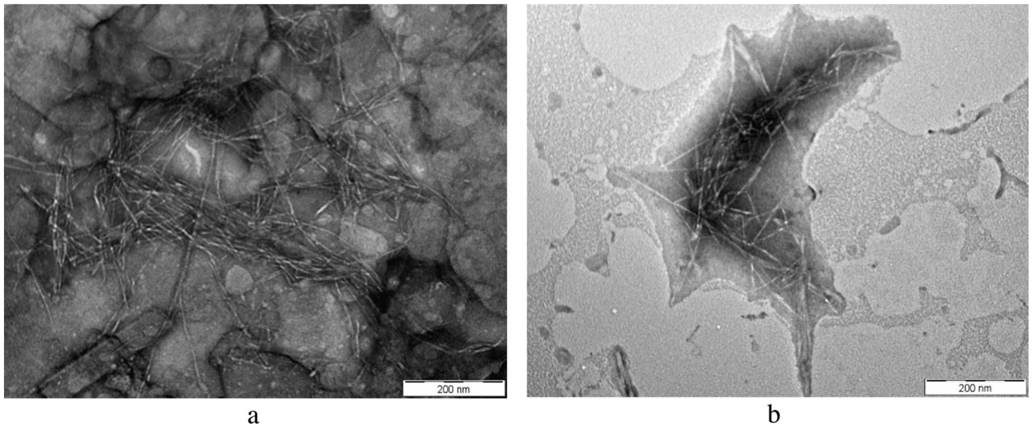

Fig. 4. Transmission electron micrographs of cellulose nanocrystals of oil palm trunk: (a) parenchyma (b) vascular bundle.

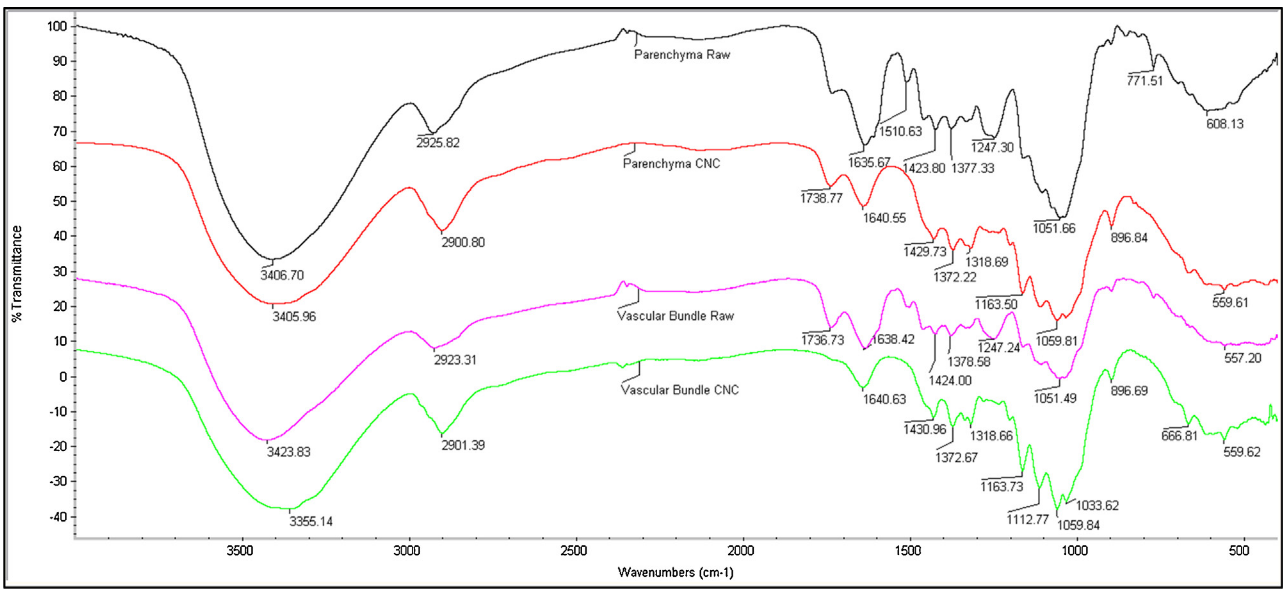

Fig. 5. FTIR spectrum of raw and cellulose nanocrystals of parenchyma and vascular bundle of oil palm trunk.

Johar, Ahmad, and Dufresne (2012), if the intensity and the position of these peaks do not changed, it means the cellulose component was not removed nor degraded after acid hydrolysis.

The IR spectra were compared with the IR spectra of raw parenchyma and the vascular bundle obtained in our previous work (Lamaming et al., 2015a). Several changes in functional groups were noticed in cellulose nanocrystals obtained after acid hydrolysis. Three major peaks at 1730–1740 cm^{-1}, 1510 cm^{-1} and 1247 cm^{-1} were prominent in the raw parenchyma and vascular bundle which correspond to the C=O linkages in lignin and hemicellulose was absent. It indicates removal of lignin and hemicelluloses and high purity of the produced cellulose nanocrystals. It is well known that

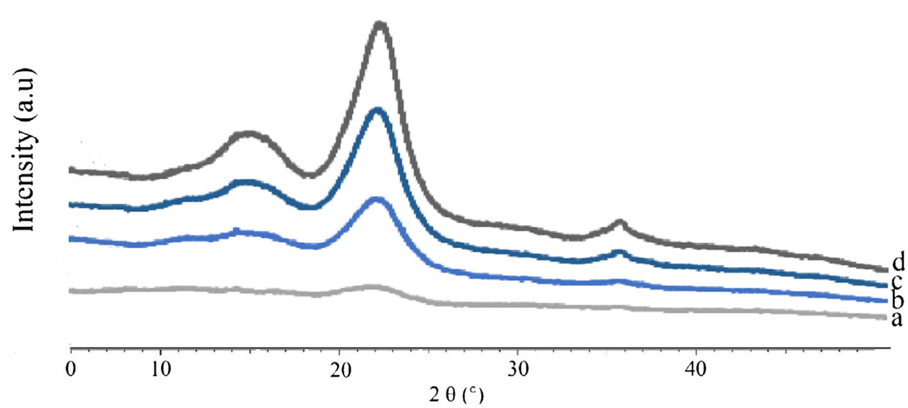

Fig. 6. X-ray curves of (a) raw parenchyma (b) raw vascular bundle and cellulose nanocrystals of (c) parenchyma and (d) vascular bundle of oil palm trunk.

the presence of lignin will interfere with the area of the crystalline peaks in the spectra (Kasprzyk & Wichlacz, 2004).

Since peak 1430 cm^{-1} assigned for crystalline, any relative shift in this peak from higher to lower frequency is an indication of cellulose degradation. The presence of 1430 cm^{-1} and 1111 cm^{-1} peak assures the sign of crystalline cellulose I form (Colom & Carillo, 2002). The peak at 897 cm^{-1} is the anomeric carbon group frequency in cellulose and hemicelluloses. Thinner peak at this peak indicates less amorphous cellulose whilst the broadening of the peak reflects higher amount of disordered structure (Proniewicz et al., 2001; Oh, Yoo, Shin, & Seo, 2005; Kavkler, Gunde-Cimerman, Zalar, & Demšar, 2011).

3.3. X-ray diffraction analysis

The degree of crystallinity is defined as the ratio of the crystalline to amorphous areas of cellulose. X-ray diffraction analysis was performed on parenchyma and vascular bundle cellulose nanocrystals to ascertain the changes in the crystallinity in the materials. Cellulose crystallinity is an important factor, determines the elasticity, rigidity, thermal stability and absorption–desorption properties of the fibers (Kasprzyk & Wichlacz, 2004). Fig. 6 displayed the X-ray curves for the parenchyma and vascular bundle cellulose nanocrystals. The presence of only one peak at $2\theta = 22°$ again confirms the crystalline cellulose of type I. Since parenchyma is living cell and plays an active role in various metabolic activities of plants, it contains high amount of moisture and water soluble compounds with low cellulose and lignin content (Mhd Ramle et al., 2012). Whereas vascular bundle is characterized as thick walled, dead cells, provides strength and transport to the plant and contains high amount of cellulose and extractives (Mhd Ramle et al., 2012). Due to this reason parenchyma exhibits much lower crystallinity index when compared to vascular bundle.

In the previous work of Lamaming et al. (2015a), the value of crystallinity index of raw parenchyma and vascular bundle was observed 18.92% and 47.47%, respectively. After acid hydrolysis, the crystallinity index of parenchyma and vascular bundle cellulose nanocrystals was observed 57.63% and 63.91%, respectively. The increase in crystallinity index is a result of the removal of amorphous lignin–hemicellulose and left behind the pure cellulose, with

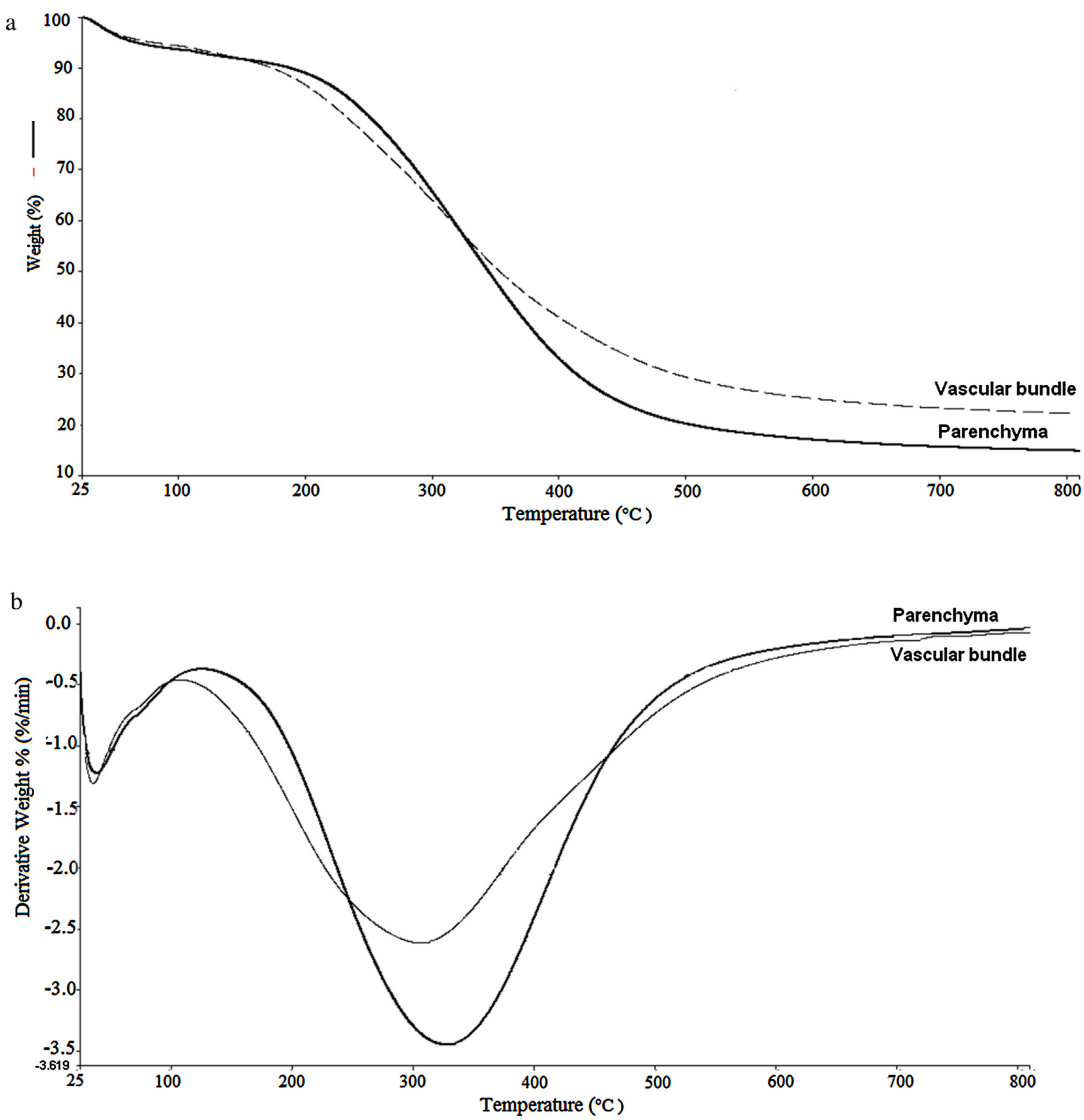

Fig. 7. Typical (a) TGA and (b) DTG curves for parenchyma and vascular bundle cellulose nanocrystals.

Table 1
Crystallinity index (%) of oil palm trunk (OPT) and cellulose nanocrystals of parenchyma and vascular bundle.

Materials	Crystallinity index (%)
OPT parenchyma	18.92
OPT vascular bundle	47.47
Cellulose nanocrystals from parenchyma	57.63
Cellulose nanocrystals from vascular bundle	63.91

204% increment for parenchyma cellulose nanocrystals. However the crystallinity index observed in the current work (Table 1) was slightly lower when compared to the previous work by Lamaming et al. (2015b) that was 68 to 70% for cellulose nanocrystals from oil palm. The reason is obvious because previously we obtained the cellulose nanocrystals from a mixture of parenchyma and vascular bundle. This would probably depends on the ratio of parenchyma and vascular bundle in OPT that we had used in our previous work.

3.4. Thermogravimetric analysis (TGA)

The TGA is performed to study the thermal stability of the cellulose nanocrystals. Fig. 7 illustrates the two stages decomposition of both cellulose nanocrystals, obtained from parenchyma and vascular bundles, respectively. In the first stage from 30 °C to 160 °C a very little weight loss was observed. According to Wielage, Lampke, Marx, Nestler, and Starke (1999), cellulose nanocrystals are quite durable up to 160 °C and little weight loss is due to the evaporation of water. Beyond 160 °C temperature, thermal stability decreases and a sharp decomposition curve is obtained.

The onset temperature was calculated at 10% degradation of cellulose nanocrystals. It was observed 257 °C and 205 °C for parenchyma and vascular bundle cellulose nanocrystals, respectively. Fig. 7b shows the DTG curves, the decomposition temperatures for cellulose nanocrystals can be analyzed from it. The cellulose nanocrystals from parenchyma show higher decomposition temperature compared to vascular bundle that is 327 °C to 309 °C, respectively. It can be pointed out that at this temperature, the cellulose in the cellulose nanocrystals began to degrade. Since the degree of crystallinity directly influences the thermal stability and mechanical properties of natural fibers, the decomposition temperature of cellulose nanocrystals was increased drastically with the increase in crystallinity index (Bruce, Bair, Vyazovkin, Gallagher, & Riga, 2008). However, both the cellulose nanocrystals were quite stable to temperature yet cellulose nanocrystals obtained from parenchyma were more stable. The reason for higher decomposition temperature for parenchyma cellulose nanocrystal was possibly due to its drastic increase in crystallinity index. The increment in crystallinity index was observed 204.5% for parenchyma whereas 34.6% for vascular cellulose nanocrystals. The onset temperature, as well as end temperature was found higher for parenchyma cellulose nanocrystals compared that of vascular bundle. The higher decomposition temperature is due to a drastic reduction in molecular weight caused by acid hydrolysis that make the materials resistant to degrade when temperature increases due to dissolving the amorphous region (Mandal & Chakrabarty, 2011; Mohamad Haafiz, Eichhorn, Hassan, & Jawaid, 2013). Not only the amorphous regions dissolves, but the acid hydrolysis also believed attacking some of the crystalline regions.

The TGA curve shows almost straight line when temperature increases above 500 °C, it is due to the presence of carbonaceous materials as remaining residue (Thiripura Sundari & Ramesh, 2012). The graph shows that the residual mass was higher (22%) on vascular bundle as compared to the parenchyma (15%). According to Mandal and Chakrabarty (2011), crystalline cellulose I have intrinsic flame resistant properties, thus a high amount of crystalline cellulose will contribute to the high residue. Similar results and pattern of the curves were observed when compared to our previous work on cellulose nanocrystals from oil palm trunk (Lamaming et al., 2015b). From the TGA curve in Fig. 7a, it was concluded that both cellulose nanocrystals have a good thermal stability.

4. Conclusions

Cellulose nanocrystals was successfully produced from the parenchyma and the vascular bundle of oil palm trunk by sulfuric acid hydrolysis method. The TEM image showed that the parenchyma cells were very long as compared to vascular bundle and observed 892.86 nm and 176.20 nm, respectively. Since the vascular bundle is believed to have higher cellulose content, the XRD result showed that vascular bundle had a higher value of crystallinity index (63.9%) compared to the parenchyma (57.63%). Thermogravimetric curves showed that both cellulose nanocrystals have a good thermal stability but it was observed higher for parenchyma cellulose nanocrystals. Since cellulose nanocrystals exhibits peculiar characteristics of shape, size, crystallinity index and thermal stability, depending on their sources, the detail study will be helpful in potential and precise application of cellulose nanocrystals. The produced cellulose nanocrystals possess multifunctional applications. The fabrication of bionanocomposite for highly sophisticated products in biomedical such as wound dressing, medicine capsule, scaffolds, and artificial limbs can be a future application.

Acknowledgements

The authors gratefully thanked Ministry of Higher Education, Malaysia for the financial support under the programme called MYBRAIN15 (Ph.D. fellowship of Junidah Lamaming), and acknowledge Universiti Sains Malaysia for the project funding under a research grant (1001/PTEKIND/811255) and Post-doctoral fellowship for Dr. Mohammed Nasir.

References

Abe, H., Murata, Y., Kubo, S., Watanabe, K., Tanaka, R., Sulaiman, O., et al. (2013). Estimation of the ratio of vascular bundle to parenchyma tissue in oil palm trunks using NIR spectroscopy. *BioResources*, *8*(2), 1573–1581.

Abraham, E., Deepa, B., Pothan, L. A., Jacob, M., Thomas, S., Cvelbar, U., et al. (2011). Extraction of nanocellulose fibrils from lignocellulosic fibres: A novel approach. *Carbohydrate Polymers*, *86*, 1468–1475.

Bakar, B. F. A., Paridah, M. T., Karimi, A., Bakar, E. S., Uyup, M. K. A., & Choo, A. C. Y. (2012). Evaluations of some physical properties of oil palm as alternative biomass resources. *Wood Material Science & Engineering*, *8*(2), 119–128.

Colom, X., & Carillo, F. (2002). Crystallinity changes in lyocell and viscose-type fibres by caustic treatment. *European Polymer Journal*, *38*, 2225–2230.

Corley, R. H. V., & Tinker, P. B. (2003). *The oil palm* (4th ed., pp. 562). Oxford UK: Blackwell Publishing Company.

Darwis, A., Nurrochmat, D. R., Massijaya, M. Y., Nugroho, N., Alamsyah, E. M., Effendi Tri Bahtiar, E. T., et al. (2013). Vascular bundle distribution effect on density and mechanical properties of oil palm trunk. *Asian Journal Plant Sciences*, *12*, 208–213.

Fahma, F., Iwamoto, S., Hori, N., Iwata, T., & Takemura, A. (2010). Isolation, preparation, and characterization of nanofibers from oil palm empty fruit bunch (OPEFB). *Cellulose*, *17*, 977–985.

Hashim, R., Nadhari, W. N. A. W., Sulaiman, O., Sato, M., Hiziroglu, S., Kawamura, F., et al. (2012). Properties of binderless particleboard panels manufactured from oil palm biomass. *BioResources*, *7*(1), 1352–1365.

Johar, N., Ahmad, I., & Dufresne, A. (2012). Extraction, preparation and characterization of cellulose fibers and nanocrystals from rice husk. *Industrial Crops and Products*, *37*(1), 93–99.

Kasprzyk, H., & Wichlacz, K. (2004). Some aspects of estimation of the crystallinity of gamma radiation wood cellulose by FTIR spectroscopy and X-ray diffraction techniques. *Acta Scientiarum Polonorum Silvarum Colendarum Ratio et Industria Lignaria*, *3*(1), 73–84.

Kavkler, K., Gunde-Cimerman, N., Zalar, P., & Demšar, A. (2011). FTIR spectroscopy of biodegraded historical textiles. *Polymer Degradation and Stability*, *96*, 574–580.

Killmann, W., & Lim, S. C. (1985). Anatomy and properties of oil palm stem. In *Proceed. Nat. Symp. On oil palm y-products for agro-based industries* Kuala Lumpur, Palm Oil Rest. Inst. Malaysia Bulletin, (pp. 18–41).

Lamaming, J., Hashim, R., Leh, C. P., Sulaiman, O., & Sugimoto, T. (2015). Chemical, crystallinity and morphological properties of oil palm trunk parenchyma and vascular bundle. *International Journal of Environmental Engineering*, *2*(1), 66–70.

Lamaming, J., Hashim, R., Sulaiman, O., Leh, C. P., Sugimoto, T., & Nordin, N. A. (2015). Cellulose nanocrystals isolated from oil palm trunk. *Carbohydrate Polymers*, *127*, 202–208.

Lim, S. C., & Khoo, K. (1986). The characteristics of oil palm trunk and its potential utilization. *Malaysian Forester*, *49*(1), 3–22.

Lim, S. C., & Fujii, T. (1997). A note on the structure of oil palm trunk by scanning electron microscopy. *Journal of Tropical Forest Products*, *3*(1), 105–109.

Mandal, A., & Chakrabarty, D. (2011). Isolation of nanocellulose from waste sugarcane bagasse (SCB) and its characterization. *Carbohydrate Polymers*, *76*, 94–99.

Mauseth, J. D. (1988). *Plant anatomy*. California: Benjamin/Cummings Publishing Co Inc.

Bruce, P. R., Bair, H. E., Vyazovkin, S., Gallagher, P. K., & Riga, A. (2008). Thermogravimetric analysis (TGA). In J. D. Menczel, & R. B. Prime (Eds.), *Thermal analysis of polymers: Fundamentals and applications* (pp. 241–317). Hoboken, NJ, USA: John Wiley & Sons Inc.

Mhd Ramle, S. F., Sulaiman, O., Hashim, R., Arai, T., Kosugi, A., Abe, H., et al. (2012). Characterization of parenchyma and vascular bundle of oil palm trunk as function of storage time. *Lignocellulose*, *1*(1), 33–44.

Mohamad Haafiz, M. K., Eichhorn, S. J., Hassan, A., & Jawaid, M. (2013). Isolation and characterization of microcrystalline cellulose from oil palm biomass residue. *Carbohydrate Polymers*, *93*, 628–634.

Oh, S. Y., Yoo, D. I., Shin, Y., & Seo, G. (2005). FTIR analysis of cellulose treated with sodium hydroxide and carbon dioxide. *Carbohydrate Research*, *340*, 417–428.

Prawitwong, P., Kosugi, A., Arai, T., Deng, L., Lee, K. C., Ibrahim, D., et al. (2012). Efficient ethanol production from separated parenchyma and vascular bundle of oil palm trunk. *Bioresource Technology*, *125*, 37–42.

Pruyn, M. L. (2007). Parenchyma. In *Handbook of plant science*. USA: John Wiley and Sons, Ltd.

Proniewicz, L. M., Paluszkiewicz, C., Weselucha-Birczyńska, A., Majcherczyk, H., Barański, A., & Konieczna, A. (2001). FT-IR and FT-Raman study of hydrothermally degradated cellulose. *Journal of Molecular Structure*, *596*, 163–169.

Segal, L., Creely, J. J., Martin, A. E., & Conrad, C. M. (1959). An empirical method for estimating the degree of crystallinity of native cellulose using the X-ray diffractometer. *Textile Research Journal*, *29*, 786–794.

Sulaiman, O., Salim, N., Nordin, N. A., Hashim, R., Ibrahim, M., & Sato, M. (2012). The potential of oil palm trunk biomass as an alternative source for compressed wood. *BioResources*, *7*(2), 2688–2706.

Thiripura Sundari, M., & Ramesh, A. (2012). Isolation and characterization of cellulose nanofibers from the aquatic weed water hyacinth—*Eichhornia crassipes*. *Carbohydrate Polymers*, *87*, 1701–1705.

Wielage, B., Lampke, Th., Marx, G., Nestler, K., & Starke, D. (1999). Thermogravimetric and differential scanning calorimetric analysis of natural fibres and polypropylene. *Thermochimica Acta*, *337*, 169–177.